

Development of a retrofit anchor system for remodeling of building exteriors

Kyu Won Yeun¹, Ki Nam Hong^{*2} and Jong Kim¹

¹Institute of Construction Technology, Seon Engineering, Cheongju, Chungbuk, Korea

²School of Civil Engineering, Chungbuk National University, Cheongju, Chungbuk, Korea

(Received April 9, 2012, Revised November 26, 2012, Accepted November 30, 2012)

Abstract. To enable remodeling of the exterior of buildings more convenient, such finishing materials as curtain walls, metal panels, concrete panels or dry stones need to be easily detached. In this respect, this study proposed a new design of the slab for the purposes. In the new design, the sides of the slab were properly modified, and the capabilities of anchors fixed in the modified slab were experimentally tested. In details, a number of concrete specimens with different sizes and compressive strengths were prepared, and the effect of anchors with different diameters and embedment depths applied in the concrete specimens were tested. The test results of the maximum capacities of the anchors were compared with the number of current design codes and the stress distribution was identified. This study found that the embedment depth specified in the current design code (ACI318-08) should be revised to be more than 1.5 times the edge distance. However, with the steel sheet reinforcement, the experiment acquired higher tensile strength than the design code proposed. In addition, for two types of specimens in the tensile strength experiment, the current design code (ACI 318-08) is overestimated for the anchor depth of 75 mm. This study demonstrated that the ideal breakout failure was attainable for the side slot details of a slab with more than 180 mm of a slab thickness and less than 75 mm of an anchor embedment depth. It is expected that these details of the modified slab can be specified in the upgraded construction design codes.

Keywords: anchor; pullout tests; failure cone; fastener; tensile capacity

1. Introduction

Building life cycles range from 20 years to more than 100 years and in some cases, they last longer than the human life cycles. Recently, the number of building remodeling case is on the rise due to the increases in the construction costs. A building remodeling is requiring a total makeover of the building surface. If the building construction methods are developed in a way allowing for an easy change of the building surface materials, the overall image of the building (and its value) may be improved a lot with the comparatively lower costs. To make this possible, it is necessary to find an easy solution for bolting the surface material to the building (Yang and Ashour 2008, Yener 1994, Yoon *et al.* 2001).

*Corresponding author, Professor, E-mail: hong@chungbuk.ac.kr

Such areas where tall buildings are located are highly valued from the commercial point of view, which means that the remodelings can be categorized as the high value-added activities. Mostly, conventional building surfaces are composed of such as curtain walls, metal panels, concrete panels, and stone materials which are attached to the building concrete by using cast-in-place anchors or post-installed anchors (Klingner and Mendonca 1982, Primavera *et al.* 1997). However, those finishings aiming at sealing the building inside from the air outside are usually not designed or constructed to be disassembled. That is, the surface and the inside of buildings are completely consolidated, such that they are not separated easily and the slots of the fixed anchors are also not reusable. In this regard, the study considers that the surface of the building might be constructed as the separate entities in the beginning stages and the flexible fixing slot might be settled by using the post-installed anchors. Meanwhile, it is also preanalysed that the position of the reinforced steel bars inside the concrete may impede the anchor attachment and devalue the quality of the work as well.

Therefore, the study preliminarily evaluates the fixing qualities of cast-in-place anchors and proposes how the building is to be designed and constructed for the post-installed anchors to be attached in a flexible and convenient way.

2. Background

2.1 Anchor system on a tall building

Fig. 1(a) is of the conventional method in which the anchor slot is cast in place, and the curtain wall is fixed to the slab with one T-type head anchor and two fasteners. The outside load is carried onto the curtain wall transom, the mullion and finally dispersed on the slab through the fasteners and the anchors.

The method above requires a large number of assembly parts and high precision works. In addition, the gaps between the joints and the finishing materials tend to causes noise between the floors, which may require any further works to seal them at the additional costs.

In Fig. 1(b), the cast-in-place slot is jointed quite poorly with the fixing part that anchors seems to be post-installed to support the load. However, the reinforced steel bar location may impede these

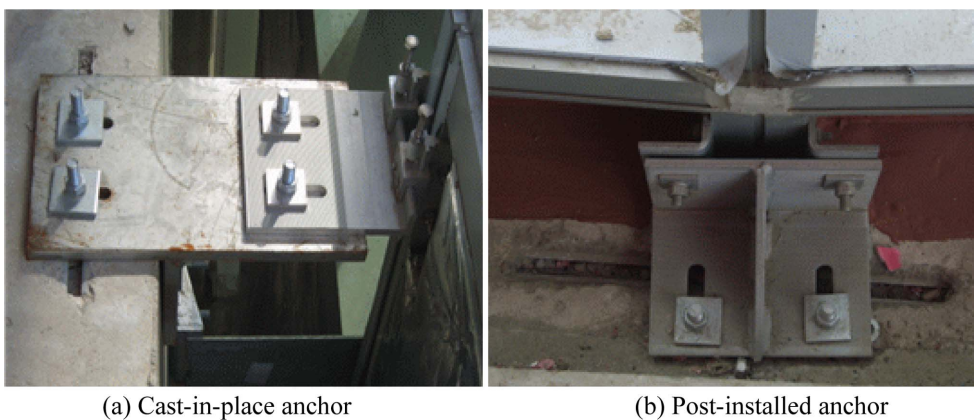


Fig. 1 Anchor systems used on tall buildings

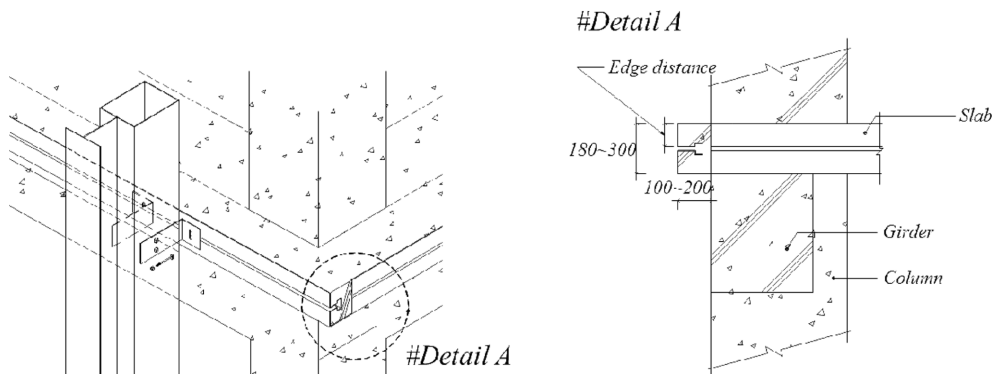


Fig. 2 Detailed view of the proposed anchor hole (unit : mm)

anchor installation, and the installation quality may be dependent on the expertise of the workers.

2.2 Proposed retrofit anchor joint part

The joining quality of the cast-in-place anchor is rather satisfactory, but the anchor doesn't look flexible in the corner, where the wind load is quite dominant. In addition, there is no room for the anchor embedments, which may need the more complicated works. By contrast, the post-installed anchors tend to present the quality problems.

To overcome these issues, the study has designed the joining structures shown in Fig. 2.

In Fig. 2, the slab protrudes outward about 100-200 mm from the column or the girder side face, and the slot on the side of the slab provides the flexible anchor-fixing locations. This design reduces the space between the finishing materials and the substrate concrete, minimizes the number of fasteners and even seals the noise between the floors.

However, the proposed anchor hole detail in Fig. 2 has a limited slab thickness. Therefore, if the anchor embedment is deep, it does not secure the required edge distances. In addition, the tensile capacity of the anchor will be severely reduced to the surface of the slot, which becomes weaker than that of the general anchor. Therefore, it appears to be difficult to calculate the load resistance capability according to the existing design code. In this respect, the study aims to present a new guideline in comparison with the design code after reviewing and analyzing the results of the experiment.

2.3 Typical tensile anchor

The most essential parts of any structural system are the connections which transfer loads between the members. Those anchors embedded in the concrete, whether they are cast-in-place or post-installed, are mostly noticed examples of such connections; they can be used to attach concrete members to structural elements.

The previous tension test data are presented in the ACI Tension Data Base, which includes both American and European results (Cook *et al.* 1992, Delhomme *et al.* 2010, Fuchs *et al.* 1995) and in the past deep anchor investigations (Lee *et al.* 2007, Peter *et al.* 1996, Stone and Carion 1983). The breakout failure of the anchor due to the tension load is composed of the ductile failure caused by

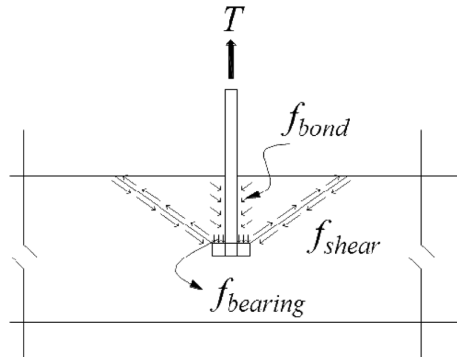


Fig. 3 Concrete breakout failure mode

the steel failure and the brittle failure caused by the concrete failure (Fuchs *et al.* 1995, Klingner and Mendonca 1982).

This study will test the tensile resistance capacities of the cast-in-place anchors at the time of concrete failure, as shown in Fig. 3.

According to Fig. 3, the concrete breaking stress is composed of the bearing stress of the anchor head, the concrete bond stress at the anchor, and the shear stress at the horizontal angle of the end of the anchor head. Early researchers (Klingner and Mendonca 1982, American Concrete Institute 1997) defined the concrete failure surface at an angle of 45° and presented the nominal capacity, which was obtained by multiplying the surface area of the truncated cone by the shear strength or the splitting tensile strength. Later, the concrete failure surface was defined by multiplying the idealized projected area by the tensile strength of the concrete.

2.4 Tension loads calculated from ACI 349-97

Under the tension loading, the concrete capacity of an arbitrary fastener is calculated by assuming a constant tensile stress equal to $0.33\sqrt{f'_c}$ (MPa) acting on the projected area of the failure cone (see Fig. 4), and by taking the inclination between the failure surface and the concrete surface as 45° , in accordance with ACI 349 (American Concrete Institute 1997)

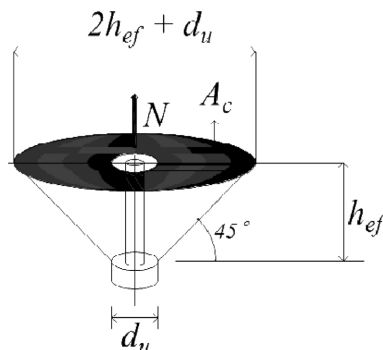


Fig. 4 Idealized concrete breakout body according to ACI 349 method

$$N = f_{ct} \times A_C \quad (1)$$

$$f_{ct} = 0.33 \sqrt{f'_c} \text{ (MPa)} \quad (2)$$

$$A_C = \pi \times h_{ef}^2 (1 + d_u/h_{ef}) \quad (3)$$

Where

N = nominal tensile capacity of anchor as governed by concrete failure (N) (see Fig. 4)

f_{ct} = constant tensile stress

A_C = projected area of stress cone (from bearing edge of anchors toward attachment)

f'_c = concrete compression strength (MPa)

h_{ef} = effective embedment depth (mm) (see Fig. 4)

d_u = nominal diameter of anchor head (mm) (see Fig. 4)

2.5 Tension loads calculated by CCD method

The concrete capacities of the arbitrary fasteners under the tension load can be calculated with the CCD method of Fuchs *et al.* (1995). Under the tension loading, the concrete capacity of a single fastener is calculated by assuming an inclination of about 35° between the failure surface and the surface of the concrete member. This corresponds to the widespread observations that the horizontal extent of the failure surface is about three times the effective embedment (Fig. 5).

The concrete cone failure load of a single anchor in the uncracked concrete unaffected by edge influences is given by Eq. (4)

$$N = k_{nc} \times \sqrt{f'_c} \times h_{ef}^{1.5} \quad (4)$$

Where

N = nominal tensile capacity of anchor as governed by concrete failure (N) (see Fig. 5)

$k_{nc} = 16.732$ for cast-in-place headed anchor bolts

f'_c = concrete compression strength (MPa).

h_{ef} = effective embedment depth (mm) (see Fig. 5)

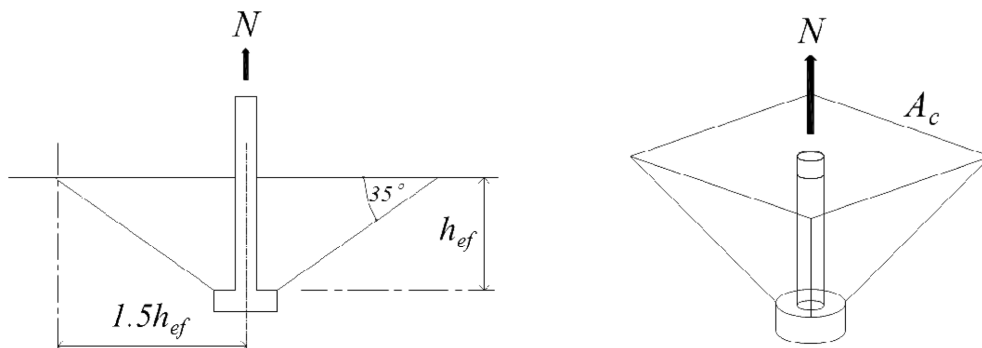


Fig. 5 Idealized concrete cone for individual fastener under tensile loading, using CCD method

2.6 Tension loads based on ACI 318-08

The recent design code, ACI 318-08 (American Concrete Institute 2008), for a uni-anchor has been updated based on experiments using the CCD method and presenting that safety is not guaranteed as the embedment depth increases

$$N = k_{nc} \times \sqrt{f'_c} \times h_{ef}^{1.5} \text{ (N)} \quad (5)$$

Where

N = nominal tensile capacity of anchor as governed by concrete failure (N) (see Fig. 5)

k_{nc} = 10 for cast-in-place headed anchor bolts

f'_c = concrete compression strength (MPa)

h_{ef} = effective embedment depth (mm) (see Fig. 5)

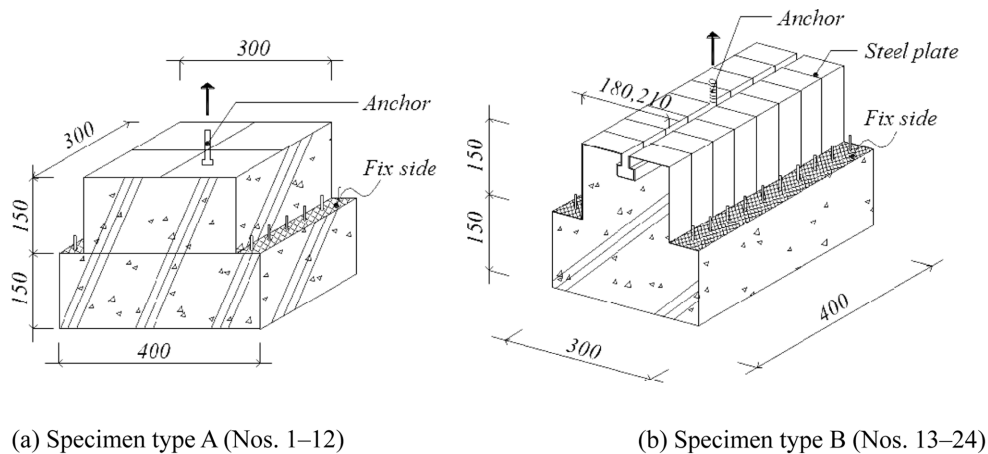
3. Experimental program

3.1 Specimen size and configuration

If the anchor is fixed to the slab side, both tensile and shear loads are working on it. The shear load for each anchor is about 5 kN, which is relatively low. It seems that the curtain wall is light in weight. However, the wind load varies according to the building height and is about 20 kN, which is shown in the structural analysis on the curtain wall.

Therefore, the embedment depth of 100 mm is acceptable, and we chose the specimen size with this in mind.

The cast-in-place anchor for the concrete takes either the yield strength of the anchor failure or the concrete breakout strength, whichever is the lower, as the design capacity. The anchor yield strength does not vary much, no matter what the materials are, but the concrete breakout strength varies according to the type of concrete, because it is basically made of the heterogeneous materials.



(a) Specimen type A (Nos. 1–12)

(b) Specimen type B (Nos. 13–24)

Fig. 6 Specimen configurations (unit : mm)

Table 1 Specimen list

No	Specimen type A list	Specimen width	Concrete strength	Anchor dia.	Anchor embedment length	No	Specimen type B list	Specimen width	Concrete strength	Anchor dia.	Anchor embedment length
		mm	MPa	mm	mm			mm	MPa	mm	mm
1	300-24-10- 50	300	24	10	50	13	180-24-10- 50	180	24	10	50
2	300-24-10- 75	300	24	10	75	14	180-24-10- 75	180	24	10	75
3	300-24-10-100	300	24	10	100	15	180-24-10-100	180	24	10	100
4	300-24-14- 50	300	24	14	50	16	180-24-14- 50	180	24	14	50
5	300-24-14- 75	300	24	14	75	17	180-24-14- 75	180	24	14	75
6	300-24-14-100	300	24	14	100	18	180-24-14-100	180	24	14	100
7	300-30-10- 50	300	30	10	50	19	200-30-10- 50	200	24	10	50
8	300-30-10- 75	300	30	10	75	20	200-24-10- 75	200	24	10	75
9	300-30-10-100	300	30	10	100	21	200-24-10-100	200	24	10	100
10	300-30-14- 50	300	30	14	50	22	200-24-14- 50	200	24	14	50
11	300-30-14- 75	300	30	14	75	23	200-24-14- 75	200	24	14	75
12	300-30-14-100	300	30	14	100	24	200-24-14-100	200	24	14	100

The strength of the joining part at the time of the concrete breakout is decided by the embedment depth of the joining part, the edge distance, and the concrete compression strength, which are mostly considered as the important factors.

According to ACI318-08, the corner distance should be 1.5 times the anchor depth. In addition, an embedment depth of 100 mm requires a slab thickness of 300 mm.

Our experiments tested two main types of specimen configurations. Specimens of type A had a standard slab thickness of 300 mm with a cast-in-place anchor, and specimens of type B had a slab thickness of either 180 or 200 mm, with 1.2-mm steel sheet reinforcement. All specimens were attached to the Universal Test Machine (UTM) by their anchors.

A total of 24 anchors were tested, including 12 cast-in-place and 12 retrofit (post-installed) anchors. Table 1 details the types of anchors tested, the concrete strength, the anchor diameter, and the embedment depth which varied between 50, 75, and 100 mm.

3.2 Specimen fixing and testing devices

To fix the specimen to the UTM, a mechanical coupler was made, as shown in Fig. 7. The stiffness is to the extent of easy assembly or disassembly and had no effect on the experiment results.

Fig. 8 shows the testing device with which we tested the tensile strength and displacement of the specimen being fixed to the UTM. For the displacement test, two 25-mm LVDTs were installed on the corner and upper surface of the concrete. The compressive strength of the anchor was not measured in the experiment because the experimental load was within the elastic limit of the anchor.

Data for the tensile load emitted by the UTM and the displacement value were received by a TDS303 and saved on a PC.

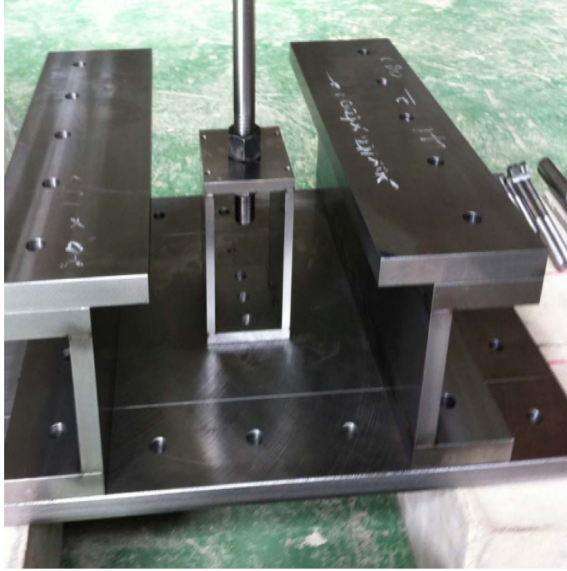


Fig. 7 Mechanical coupler



Fig. 8 Test setup of loading system

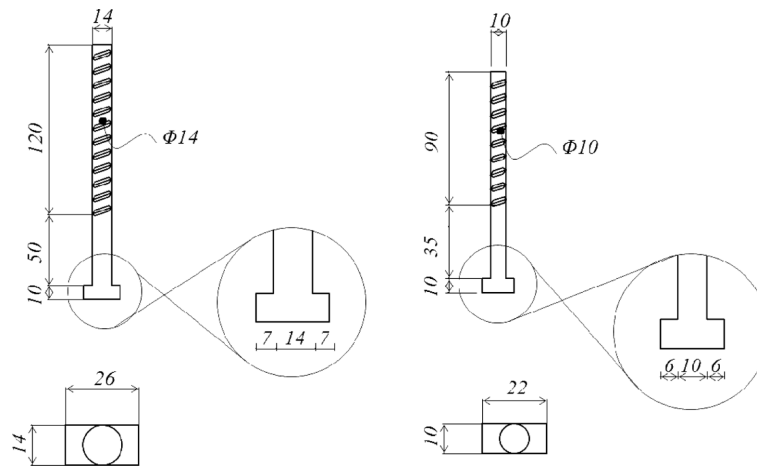


Fig. 9 Details of tested anchors (unit : mm)

3.3 Details of anchors

The anchor's sustaining capability of the building surface is within 20 kN. Therefore, the anchor diameters used were $\Phi 10$ mm and $\Phi 14$ mm. The anchor strength was 400 MPa and the Poisson's ratio was 0.3, and it was made as in Fig. 9. The cast-in-place anchors buried in specimens of type A were made of the conventional materials. The anchor head was made in a size that resists pressure breaking and in a shape that was easily to be installed into the slot. The anchor head was made of the same material to prevent the intrinsic tensile breaking.

3.4 Material properties of concrete

Two types of concrete were cast. Both were placed in the steel molds. The mixture proportion of concretes and their slump are summarized in Table 2.

In the experiment, ordinary Portland cement (density: 315 kg/m³, fineness: 3265 cm²/g), natural sand (density: 256 kg/m³), and crushed aggregate with 20 mm maximum size (density: 267 kg/m³) were used.

All aggregate was used in the saturated surface-dry condition. In addition, for the mixing agents of SP and AE, polycarbon acid series and vinsol series were used.

Concrete mixing was achieved by the use of a fan-type mixer; a diagram of the process is shown in Fig. 10. The mixing amount was 20 liters at once and repeated several times and the concrete was covered by vinyl during a curing period as shown in Fig. 11.

Table 2 Concrete mixtures and slump results

	Type I concrete	Type 2 concrete
ASTM Type I cement (kg/ m ³)	360	383
Siliceous sand (kg/m ³)	361	770
Pea gravel, 20-mm (kg/m ³)	971	942
Water (kg/m ³)	180	180
Water-cement ratio	50	47
Slump (mm)	170	180

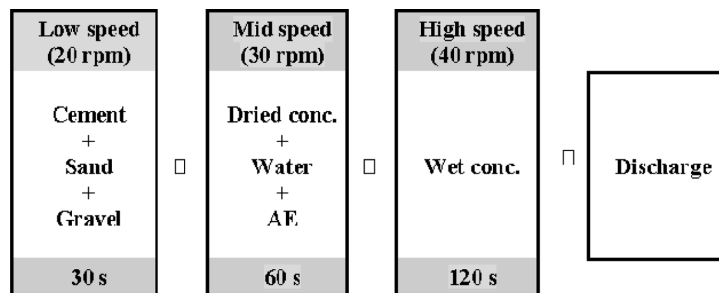


Fig. 10 Concrete mixing



Fig. 11 Fan-type mixer and curing

For fresh concrete, slump was tested. For hardened concrete, tests of compressive strength and tensile strength were carried out with cylindrical specimens of 100 mm in size after 28 days.

4. Experimental results

4.1 Compressive strength and splitting tensile strength of concrete

For the case where the tensile strength capacity of the anchor is decided by the concrete breakout, the theoretical formula shows that the compressive strength and the tensile strength are very influential. Therefore, we performed experiments to test the compressive and splitting tensile strengths. The splitting tensile strength value can be compared to the break range with the help of the main compressive strength's marginal value.

The test results showed that the specimens had compressive strengths of 27.8 MPa and 30.1 MPa, respectively. The splitting tensile strength test results showed that the specimens had splitting tensile strengths of 2.7 MPa and 2.9 MPa, respectively. Therefore, the splitting tensile strength was roughly 10% of the compressive strength.

4.2 Comparison of design methods with experimental results

Table 3 lists the test results and the calculations using three design codes. The tensile capacities calculation using the design code did not consider the strength reduction factors in the comparison with the experimental ultimate loads.

In Table 3, the tensile capacities recorded were more than the design tension loads in both specimen types A and B, which prove that the open hole does not affect the tensile capacities. This is because the open hole was reinforced by the 1.2-mm steel sheet, and the anchor head was made in the bigger size. Therefore, the recently proposed code ACI 318-08 is applicable to the details of the study.

Table 3 Summary of anchor tests and comparison with ACI and CCD results

No.	Specimen type A list	Ultimate load	CCD-95	ACI 349-97	ACI 318-08	No.	Specimen type B list	Ultimate load	CCD-95	ACI 349-97	ACI 318-08
		kN	kN	kN	kN			kN	kN	kN	kN
1	300-24-10- 50	34.1	29.0	17.0	17.3	13	180-24-10- 50	25.0	29.0	17.0	17.3
2	300-24-10- 75	50.3	53.2	35.1	31.8	14	180-24-10- 75	36.0	53.2	35.1	31.8
3	300-24-10-100	60.1	82.0	59.4	49.0	15	180-24-10-100	43.2	82.0	59.4	49.0
4	300-24-14- 50	29.4	29.0	18.3	17.3	16	180-24-14- 50	30.0	29.0	18.3	17.3
5	300-24-14- 75	43	53.2	37.0	31.8	17	180-24-14- 75	41.6	53.2	37.0	31.8
6	300-24-14-100	55.4	82.0	62.0	49.0	18	180-24-14-100	47.8	82.0	62.0	49.0
7	300-30-10- 50	26.6	32.4	19.0	19.4	19	200-24-10- 50	33.2	29.0	17.0	17.3
8	300-30-10- 75	52.8	59.5	39.2	35.6	20	200-24-10- 75	43.5	53.2	35.1	31.8
9	300-30-10-100	56	91.6	66.5	54.8	21	200-24-10-100	55.3	82.0	59.4	49.0
10	300-30-14- 50	35.8	32.4	20.4	19.4	22	200-24-14- 50	30.3	29.0	18.3	17.3
11	300-30-14- 75	44.9	59.5	41.3	35.6	23	200-24-14- 75	46.9	53.2	37.0	31.8
12	300-30-14-100	54.9	91.6	69.3	54.8	24	200-24-14-100	56.3	82.0	62.0	49.0

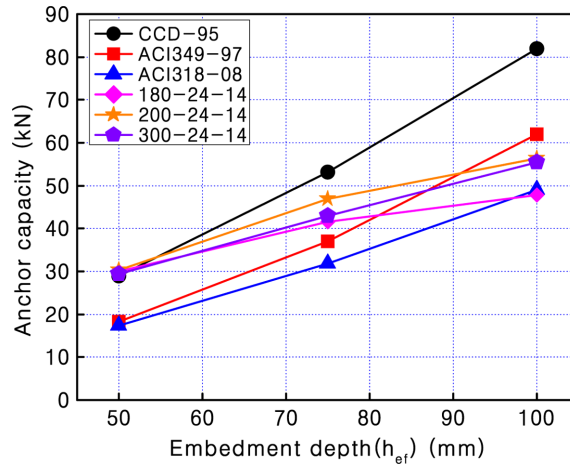


Fig. 12 Comparison of test data with ACI and CCD values for $\Phi 14$ anchor

Fig. 12 is a graph comparing the anchor embedment depth to the anchor tensile strength. The CCD-95 code requires too high a tensile strength and ACI318-08 seems too conservative as well.

In the graph, we see similar results for the anchor embedment of 75 mm and slab thicknesses of 200 and 300 mm. But with the slab thickness of 180 mm, the tensile strength has a slightly lower value. With an embedment depth of 100 mm, ACI318-08 is satisfied, even the tensile strength is lowered. Thus, the following additional research is recommended.

4.3 Experimental results for load-displacement relations

Fig. 13 displays the load-displacement relations at the anchor depth of 50 mm. At the initial stage of the test, the results of all specimens were similar. However, above the 10-kN load, it varies because of the fracture.

The tensile strength was not affected by the anchor depth of 50 mm and the slab thickness of more than 180 mm, but with depths of 75 and 100 mm, the displacement was difficult to test

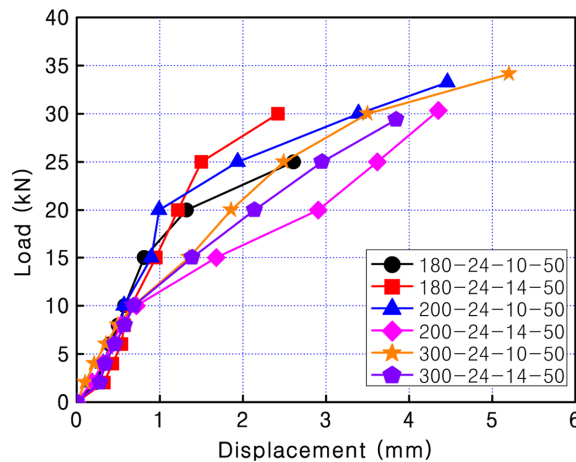


Fig. 13 Load-displacement relations at anchor depth of 50 mm

because of the displacement occurring at the testing position.

4.4 Failure mode as a function of embedment depth

All experimental members were decided based on the brittle failures but the anchor yielding has not occurred. The peak load corresponded to the concrete breakout and was defined as the anchor tensile capacity.

In Fig. 14, specimens of type A with anchor depths of 50 and 75 mm showed the stable cracking pattern, but specimens of type A with a 100-mm depth required more than 300 mm slab thickness, which was more than 1.5 times the anchor depth. Specimens of type B with anchor depths of 75 and 100 mm had a lower-than-expected failure capacity because of the errors and the eccentric loads.



(a) Specimen type A (50-mm embedment)



(b) Specimen type B (50-mm embedment)



(c) Specimen type A (75-mm embedment)



(d) Specimen type B (75-mm embedment)



(e) Specimen type A (100-mm embedment)



(f) Specimen type B (100-mm embedment)

Fig. 14 Cracking patterns for specimen types A and B

Therefore, the anchor depth of 100 mm requires a slab thickness of more than 300 mm unless it is reinforced structurally.

5. Finite element analysis

In the engineering practice, the headed anchors are often used to transfer loads into the reinforced concrete (Yoon *et al.* 2001, Klingner and Mendonca 1982, Primavera *et al.* 1997). A large number of experiments and numerical studies with anchors of different sizes confirm that the fasteners are capable of transferring the tension forces into the concrete members without the need for reinforcement (Ozbolt *et al.* 2007, Matthew *et al.* 2008). To better understand the crack growth and to predict the concrete cone failure load of the headed

anchors for the different embedment depths, a number of experimental and theoretical studies have been carried out (Kang *et al.* 2010, Matthew *et al.* 2008, McMackin *et al.* 1973, Yang and Ashour 2008, Yener 1994).

With the slab thickness of less than 180 mm, the anchor embedment depth of 50 mm has acquired the enough tensile capacity. However, for the experiment with the anchor depth of 75 mm, the additional three-dimensional finite element (FE) analysis has been done to evaluate the safety and protect against local failure due to the specimen production errors and the experimental errors.

The FE analysis on the anchor depth of 100 mm was excluded from the study because the case requiring structural reinforcement was demonstrated above.

5.1 Analytical model

To review the failure behavior of the concrete, we have analyzed the 3 specimens which are applicable to the actual building structure.

For each anchor, two embedment depths were used (50 and 75 mm). The properties of analysis data for all the investigated cases are summarized in Tables 4 and 5. The applied load in Table 4 was used based on the pull-out capacity, which was acquired by the testing results. The concrete properties were taken as Young's modulus $E_c = 28,700$ MPa, Poisson's ratio $\nu_c = 0.167$, tensile strength $f_t = 3.0$ MPa, and uniaxial compressive strength $f_c = 27$ MPa. The behavior of steel was assumed to be linear elastic with Young's modulus $E_s = 505,940$ MPa and Poisson's ratio $\nu_s = 0.3$.

Table 4 Analysis specimens

No	Specimen list	Applied load (kN)
1	180-24-14-50	30
2	180-24-14-75	42
3	300-24-14-75	43

Table 5 Properties of analysis materials

	Anchor/Steel plate	Concrete
Young's modulus (MPa)	505,940 (SM400)	28,700 (27MPa)
Poisson's ratio	0.3	0.167

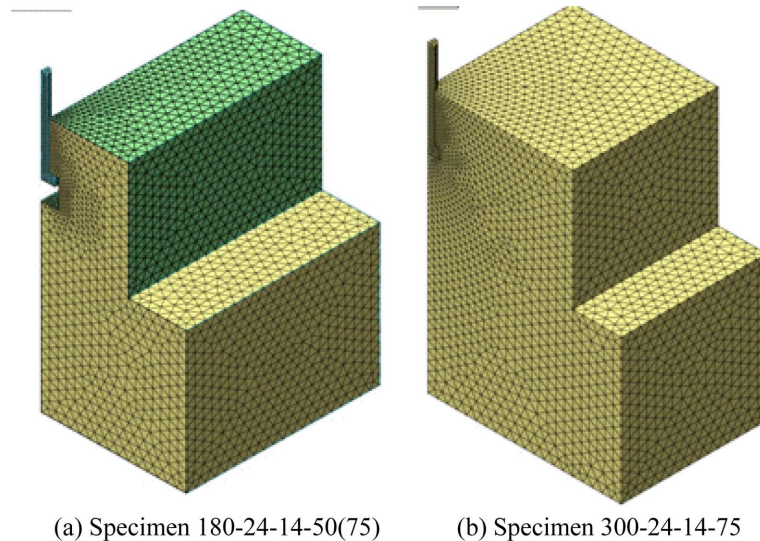


Fig. 15 Analytical model

The FE code employed in the present study was developed for three-dimensional nonlinear analysis of the structures made of the brittle materials such as concrete. The spatial discretization was performed using four- or eight-node solid finite elements (Fig. 15). The analysis was carried out incrementally; i.e. the load was applied in several steps. The preparation of the input data (pre-processing) and the evaluation of the numerical results (post-processing) were performed using the commercial program NEi Nastran FX Professional (NEi Software, Inc., Westminster, CA).

Only one-quarter of the concrete block was modeled, and double symmetry was utilized. The typical FE meshes of concrete block and the headed anchor are shown in Fig. 15. The contact between the steel anchor and the concrete exists at the top of the head of the anchor (compression transfer zone) and the stem. The analysis model was split into 3-mm intervals around the anchors as per Fig. 15, and into 10-mm intervals for other insignificant areas, to reduce the analysis time.

In addition, because the open hole at the anchor location area in Fig. 15(a) may lead to the large deformity, we have utilized the nonlinear geometry analysis.

In general, the tensile strength of the concrete was one-tenth of the compressive strength. Thus, the structure where the tensile load was acting was not considered in the material nonlinear analysis because the structure was assumed to be an elastic material.

5.2 Finite element analysis results

Figs. 16 to 18 show the compressive and tensile stresses of the concretes when the tensile stress acts on the anchor.

Fig. 16 shows the principal stress distribution of the analysis result on the slab with a thickness of 300 mm, anchor of $\Phi 14$ mm diameter, and embedment depth of 75 mm. The compressive stress formed mainly on the joining parts and the results were higher than that on the upper part of the anchor head. The tensile stress was the largest on the anchor head, but the fracture line was predicted from the anchor head to the member supporting points.

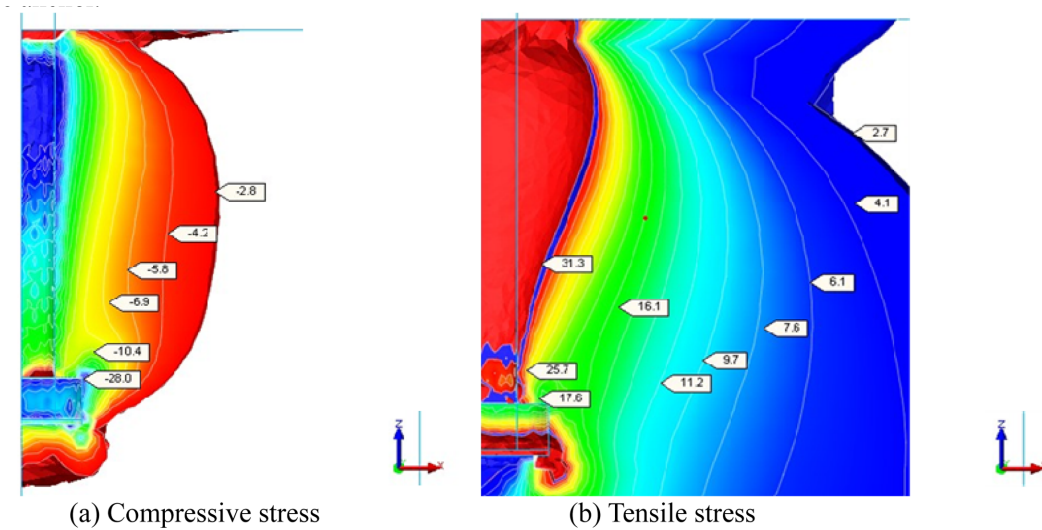


Fig. 16 Principal stresses (MPa) on specimen 300-24-14-75

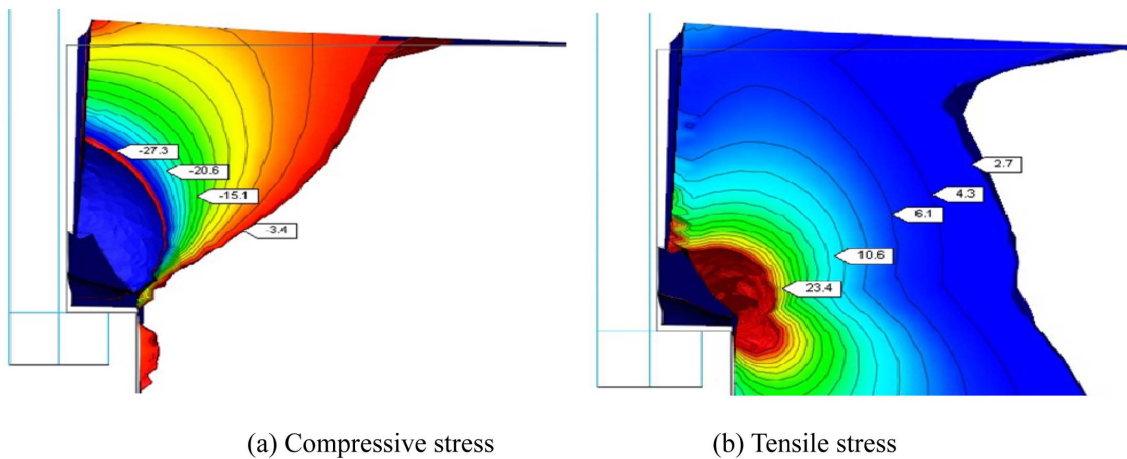
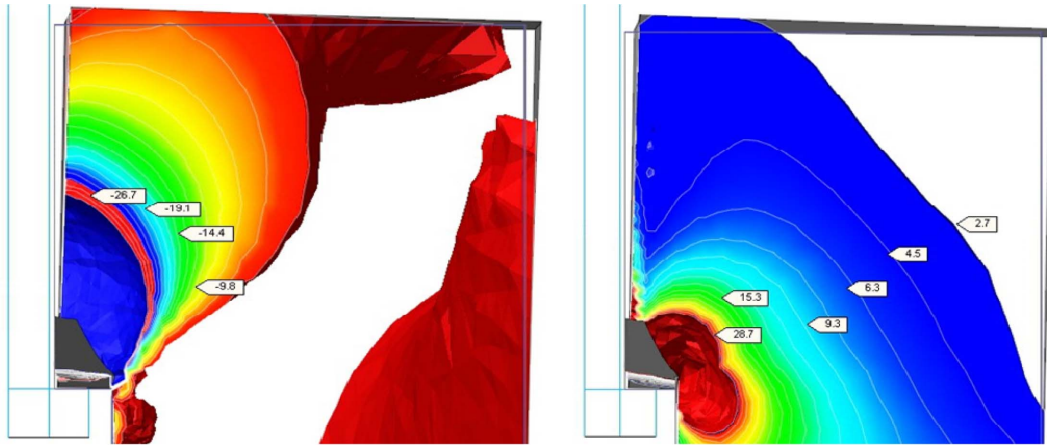


Fig. 17 Principal stresses (MPa) for specimen 180-24-14-50

Fig. 17 shows the principal stress distribution of the analysis result on the slab with a thickness of 180 mm, anchor of $\Phi 14$ mm diameter, and embedment depth of 50 mm.

The compressive stress in Fig. 17(a) demonstrates the different distribution from Fig. 16(a) as the joint is separated. The stress distribution on the anchor head was greater than the compressive stress of the concrete of 27 MPa and therefore, leads to bearing failure. Fig. 17(b) shows the area where the tensile stress was more than 2.7 MPa and the failure line forms at about 45° angle based on the anchor head.

Fig. 18 shows the principal stress distribution of the analysis result on a slab which is similar to those in Fig. 17, except for the fact that the embedment depth was 75 mm. The compressive stress in Fig. 18(a) is similar to that of Fig. 17(a), but the tensile stress in Fig. 17(b) is larger than the stress distribution and extended to the supporting points.



(a) Compressive stress

(b) Tensile stress

Fig. 18 Principal stresses (MPa) on specimen 180-24-14-75

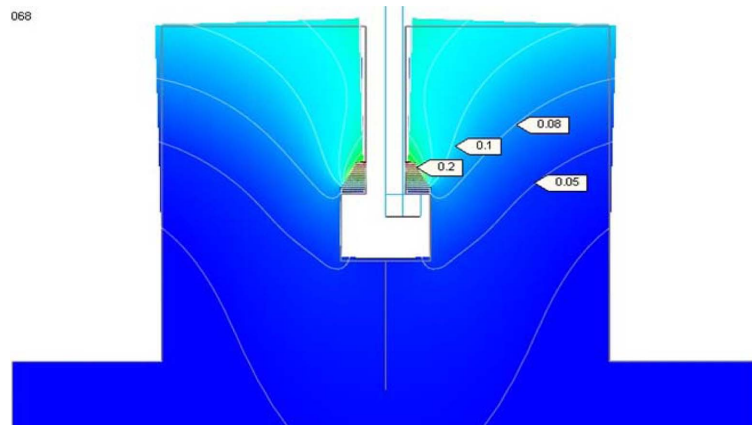


Fig. 19 Displacement contour line (mm) for specimen 180-24-14-75

Therefore, the slab thickness of 180 mm and the embedment depth of more than 75 mm are not suitable for the joint details.

Fig. 19 demonstrates the displacement analysis on the slab of 180 mm thickness with a slot of 75-mm depth. The maximum displacement occurred on the anchor head, and it formed a contour line as the distance from the anchor increased.

The result was analyzed by the geometrical nonlinear analysis, but the analytical results were less than the actual displacement. However, the displacement distribution was similar to the experimental result.

6. Conclusions

We have developed an advanced fixing structure for attaching various finishing materials to a

building and tested the structure's capabilities. From our analysis of the experimental results, the study concludes as follows. Firstly, the existing design code (ACI318-08) requires the embedment depth to be more than 1.5 times the edge distance. However, with the steel sheet reinforcement, the experiment has acquired the higher tensile strength than the design code proposes. Secondly, for two types of specimen in the tensile strength experiment, the current design code (ACI 318-08) seems to be overly safe within 75 mm of anchor depth, which needs to be properly modified. Finally, the study presents that the ideal breakout failure is attainable for the side slot details of a slab with more than 180 mm of a slab thickness and less than 75mm of anchor embedment depth. These details are applicable to the construction design regulated by the design code.

Acknowledgments

The work presented in this paper was funded by the Building-Façade Maintenance Robot Research Center (BMRC), supported by the Korea Institute of Construction and Transportation Technology Evaluation and Planning (KICTEP) under the Ministry of Land, Transport and Maritime Affairs (MLTM).

References

- American Concrete Institute (2008), "Building code requirements for structural concrete (ACI 318-08) and commentary", ACI Committee 318, American Concrete Institute, 409-438.
- American Concrete Institute (1997), "Code requirements for nuclear safety related concrete structures (ACI 349-97)", ACI Committee 349, American Concrete Institute, 123.
- Cook, R.A., Collins, D.M., Klingner, R.E. and Polyzois, D. (1992), "Load-deflection behavior of cast-in-place and retrofit concrete anchors", *ACI Struct. J.*, **89**, 639-649.
- Delhomme, F. and Debicki, G. (2010), "Numerical modeling of anchor bolts under pullout and relaxation tests", *Constr. Buil. Mater.*, **24**, 1232-1238.
- Delhomme, F., Debicki, G. and Chaib, Z. (2010), "Experimental behaviour of anchor bolts under pullout and laxation tests", *Constr. Buil. Mater.*, **24**, 266-274.
- Fuchs, W., Eligehausen, R. and Breen, J.E. (1995), "Concrete capacity design (CCD) approach for fastening to concrete", *ACI Struct. J.*, **92**, 73-94.
- Kang, T.K., Ha, S.S. and Choi, D.U. (2010), "Bar pullout tests and seismic tests of small-headed bars in beam-column joints", *ACI Struct. J.*, **107**, 32-42.
- Klingner, R.E. and Mendonca, J.A. (1982), "Tensile capacity of short anchor bolts and welded studs: A literature review", *ACI Struct. J.*, **79F**, 270-279.
- Lee, N.H., Kim, K.S., Bang, C.J. and Park, K.R. (2007), "Tensile-headed with large diameter and deep embedment in concrete", *ACI Struct. J.*, **104**, 479-486.
- Hoehler, M.S. and Eligehausen, R. (2008), "Behavior and testing of anchors in simulated seismic cracks", *ACI Struct. J.*, **105**, 348-357.
- Matthew S. Hoehler and Rolf Eligehausen (2008), "Behavior and testing of anchors in simulated seismic cracks", *ACI Struct. J.*, **105**, 348-357.
- McMackin, P.J., Slutter, R.G. and Fisher, J.W. (1973), "Headed steel anchors under combined loading", *AISC Eng. J.*, Second Quarter, 43-52.
- Ozbolt, J., Eligehausen, R., Periskic, G. and Mayer, U. (2007), "3D FE analysis of anchor bolts with large embedment depths", *Constr. Buil. Mater.*, **74**, 168-178.
- Peter, J.C., Kurt, W.K. and Jai, B.K. (1996), "Tension test of heavy-duty anchors with embedments of 8 to 19 inches", *ACI Struct. J.*, **93**, 360-368.

- Primavera, E.J., Pinelli, J.P. and Kalajian, E.H. (1997), "Tensile behavior of cast-in-place and undercut anchors in high-strength concrete", *ACI Struct. J.*, **94**, 583-594.
- Stone, W.C. and Carion, N.J. (1983), "Deformation and failure in large-scale pullout tests", *ACI Struct. J.*, **80**, 501-512.
- Yang, K.H. and Ashour, A.F. (2008), "Mechanism analysis for concrete breakout capacity of single anchors in tension", *ACI Struct. J.*, **105**, 609-616.
- Yener, M. (1994), "Overview and progressive finite element analysis of pullout tests", *ACI Struct. J.*, **91**, 49-58.
- Yoon, Y.S., Kim, H.S. and Kim, S.Y. (2001), "Assessment of fracture behaviors for CIP anchors fastened to cracked and uncracked concretes", *KCI Concrete J.*, **13**, 33-41.